

High-fidelity conversion of photonic quantum information to telecommunication wavelength with superconducting single-photon detectors

Rikizo Ikuta,¹ Hiroshi Kato,¹ Yoshiaki Kusaka,¹ Shigehito Miki,² Taro Yamashita,² Hirotaka Terai,² Mikio Fujiwara,³ Takashi Yamamoto,¹ Masato Koashi,⁴ Masahide Sasaki,³ Zhen Wang,² and Nobuyuki Imoto¹

¹*Graduate School of Engineering Science, Osaka University, Toyonaka, Osaka 560-8531, Japan*

²*Advanced ICT Research Institute, National Institute of Information and Communications Technology (NICT), 588-2 Iwaoka, Kobe 651-2492, Japan*

³*Advanced ICT Research Institute, National Institute of Information and Communications Technology (NICT), 4-2-1 Nukuikawa, Koganei, Tokyo 184-8795, Japan*

⁴*Photon Science Center, The University of Tokyo, Bunkyo-ku, Tokyo 113-8656, Japan*

(Received 2 July 2012; published 2 January 2013)

We experimentally demonstrate a high-fidelity visible-to-telecommunication wavelength conversion of a photon by using a solid-state-based difference frequency generation. In the experiment, one half of a picosecond visible entangled photon pair at 780 nm is converted to a 1522-nm photon, resulting in the entangled photon pair between 780 and 1522 nm. Using superconducting single-photon detectors with low dark count rates and small timing jitters, we selectively observed well-defined temporal modes containing the two photons. We achieved a fidelity of 0.93 ± 0.04 after the wavelength conversion, indicating that our solid-state-based scheme can be used for faithful frequency down conversion of visible photons emitted from quantum memories composed of various media.

DOI: [10.1103/PhysRevA.87.010301](https://doi.org/10.1103/PhysRevA.87.010301)

PACS number(s): 42.50.Ex, 03.67.Hk, 42.50.Dv, 42.65.Ky

Wavelength conversion of photons in a quantum regime [1] has been actively studied [2–10] as a quantum interface for the application of quantum information processing and communications. Especially, such a conversion, aiming at near-infrared photons in telecommunication bands, is essential for transmitting quantum information over long-distance optical fiber networks with quantum repeaters [11–13]. In the quantum repeaters, the photon sent to a relay point through an optical fiber needs to be entangled with a quantum memory. At present, many of quantum memories and processors based on alkaline atoms, trapped ions, and solid states have successfully created entanglement with photons at around visible wavelengths [14–20]. Thus, a quantum interface for the wavelength conversion from visible to telecommunication bands with a high fidelity has attracted much interest for its applications. So far, such a quantum interface has been demonstrated by using four-wave mixing with a cold-atomic cloud [6] or difference frequency generation (DFG) from a nonlinear optical crystal [7]. Among them, nonlinear optical crystals with waveguide structures have practically desirable features. They can operate near room temperature and do not require a laser-cooling configuration, enabling a compact setup and integration into a photonic quantum circuit on a chip using waveguide structures [21]. In addition, they have a wider bandwidth, compatible with wideband quantum memories [22,23], resulting in high-clock-rate quantum information processing. Such kinds of solid-state-based optical quantum interfaces lead to the development of a mature quantum information technology. However, in several demonstrations of the solid-state-based wavelength conversion [4,7,24–26], they suffered from degradation of an observed fidelity of a reconstructed quantum state after the wavelength conversion due to background noises caused by Raman scattering of a strong cw pump light and relatively high dark count rate of an InGaAs/InP avalanche photodiode (APD) for photon

detection at the telecommunication band. Therefore, the observed fidelity of the state, after the wavelength conversion, is degraded.

In this Rapid Communication, we demonstrate almost noiseless wavelength conversion by suppressing the effects of both the optical noise from the Raman scattering and the dark count via newly developed superconducting single-photon detectors (SSPDs) for visible and telecommunication wavelengths of the photons [27,28]. The SSPDs have lower dark count rates and smaller timing jitters than those of typical APDs. Especially, the latter property enables us to selectively observe well-defined temporal modes containing the two photons. Because duration of signal photons in our experiment is of picosecond order, whereas, the optical noise through the wavelength conversion is continuously generated, the use of the SSPDs leads to the reduction in irrelevant photon detections. The observed fidelity of the two-photon state, after the wavelength conversion to a maximally entangled state, is 0.93 ± 0.04 , which is very close to the initial fidelity of 0.97 ± 0.01 . We also clearly observe the violation of the Clauser-Horne-Shimony-Holt-type Bell's inequality with $S = 2.62 \pm 0.09$.

Theoretical treatment of wavelength conversion of a single mode of a pulsed light is as follows [1,7]. When a pump light at angular frequency ω_p is sufficiently strong, the Hamiltonian of the wavelength conversion using a second-order nonlinear optical interaction is described by $\hat{H} = i\hbar\sqrt{\eta P}(e^{-i\varphi}\hat{a}_s^\dagger\hat{a}_s - e^{i\varphi}\hat{a}_s^\dagger\hat{a}_c)$. Here, \hat{a}_s and \hat{a}_c are annihilation operators of a signal mode at angular frequency ω_s and a converted mode at angular frequency $\omega_c = \omega_s - \omega_p$, respectively. P and φ are a power and a phase of the classical pump light, respectively. η is a constant, and $\sqrt{\eta P}e^{i\varphi}$ represents an effective coupling constant. Using this Hamiltonian, an annihilation operator $\hat{a}_{c,\text{out}}$ of the converted mode, coming from the nonlinear optical crystal, is described by using the time evolution of \hat{a}_s in the

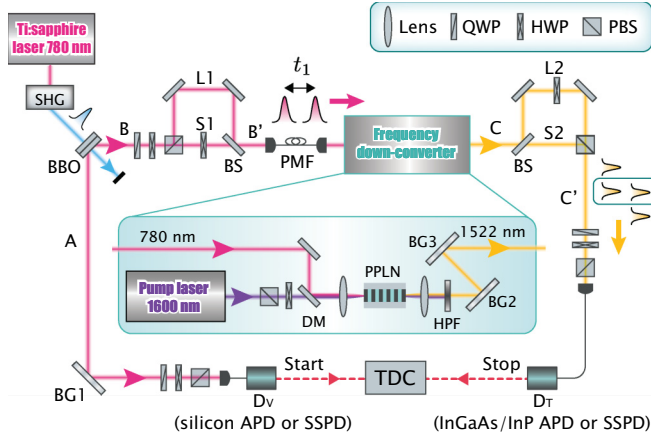


FIG. 1. (Color online) The experimental setup for frequency down conversion of one half of the visible entangled photon pairs.

Heisenberg picture as

$$\hat{a}_{c,\text{out}} = \hat{a}_c(\tau) = e^{-i\varphi} \sin(\sqrt{\eta P \tau}) \hat{a}_s + \cos(\sqrt{\eta P \tau}) \hat{a}_c, \quad (1)$$

where τ is the traveling time of the pulses through the crystal.

The experimental setup for the DFG-based frequency down conversion of one half of a polarization-entangled photon pair at 780 nm to the wavelength of 1522 nm is shown in Fig. 1. We use a mode-locked Ti:sapphire laser (wavelength: 780 nm; pulse width: 1.2 ps; repetition rate: 82 MHz) as a light source. It is frequency doubled by a second-harmonic generator (SHG), and then the UV pulse with a power of 250 mW pumps a pair of type-I phase-matched 1.5-mm-thick β -barium borate (BBO) crystals to prepare the polarization-entangled photon pair A and B , which is described as $|\phi^+\rangle_{AB} \equiv (|HH\rangle_{AB} + |VV\rangle_{AB})/\sqrt{2}$ through spontaneous parametric down conversion [29]. Here, $|H\rangle$ and $|V\rangle$ represent horizontal (H) and vertical (V) polarization states of a photon. The spectrum of photon A is narrowed by a Bragg grating (BG1) with a bandwidth of 0.2 nm, and then the photon is detected by detector D_V , connected to a single-mode fiber. We switch the silicon APD and the SSPD for D_V . Photon B is split into a short path ($S1$) and a long path ($L1$) according to a polarization of the photon. A half-wave plate (HWP) in $S1$ flips the polarization from H to V . As a result, a polarization qubit $\{|H\rangle, |V\rangle\}$ in mode B is transformed to a time-bin qubit $\{|S1\rangle, |L1\rangle\}$ in mode B' , leading to a two-photon state in modes A and B' of $|\psi\rangle_{AB'} \equiv (|H\rangle_A |S1\rangle_{B'} + |V\rangle_A |L1\rangle_{B'})/\sqrt{2}$. Here, $|S1\rangle$ and $|L1\rangle$ represent states of V -polarized photons passing through $S1$ and $L1$, respectively. We set the time difference between $S1$ and $L1$ to about 700 ps. The photon in mode B' goes through a polarization-maintaining fiber (PMF) and then enters the frequency down converter whose details are shown in the inset of Fig. 1.

For the DFG of the signal photon at 780 nm, a cw pump laser at 1600 nm is used. The linewidth of the pump light is 150 kHz, and its coherence time is much longer than the time difference of the photons passing through $S1$ and $L1$. The pump light is combined with the signal photon at a dichroic mirror (DM) after its polarization is set to V by a polarization beam splitter (PBS) and a HWP. Then, they are focused on the type-0 quasi-phase-matched ($V \rightarrow V + V$)

periodically-poled lithium niobate (PPLN) waveguide [30] whose temperature is controlled to be about 50 °C. The length of the PPLN crystal is 20 mm, and the acceptable bandwidth is calculated to be about 0.3 nm. After passing through the PPLN waveguide, the strong pump light is diminished by a high-pass filter (HPF), and the light, converted to the wavelength of 1522 nm, is extracted by BG2 and BG3 whose bandwidths are 1 nm.

The photon in mode C from the frequency down converter is split into a short path ($S2$) and a long path ($L2$) by a BS. The polarization of the photon passing through $L2$ is flipped from V to H by a HWP. The time difference between $S2$ and $L2$ is adjusted to be the same as that between $S1$ and $L1$. The components of the photon from $S2$ and $L2$ are recombined by a PBS, and the photon in mode C' is detected by D_T after passing through a single-mode fiber. We switch the InGaAs/InP APD and the SSPD for D_T .

Each SSPD consists of an 100-nm-thick Ag mirror, a $\lambda/4$ SiO cavity, and a 4-mm-thick niobium nitride meander nanowire on a 0.4-mm-thick MgO substrate from the top. The nanowire is 80-nm wide, and it covers an area of $15 \mu\text{m} \times 15 \mu\text{m}$. The respective optical cavity structures of the SSPDs for D_V and D_T are designed for visible and telecommunication wavelengths to achieve higher detection efficiencies. The detection efficiencies are 32% and 12.5% for 780- and 1522-nm wavelengths, respectively. Each of the SSPD chips is shielded by a copper block, which has a holder of a single-mode optical fiber followed by a small-gradient index lens for efficient coupling. The blocks are installed in the Gifford-McMahon cryocooler system whose cooling temperature is 2.28 ± 0.02 K.

To measure the coincidence events of the detections at D_V and D_T , signals from D_V and D_T are input to a time-to-digital converter (TDC) as a start and stop signal of a clock, respectively. By postselecting the events where the photon in mode C' has passed through $S1$ - $L2$ or $L1$ - $S2$, we obtain the polarization-entangled state $|\phi^+\rangle_{AC'}$ in modes A and C' . In our experiment, we accept such events in a 200-ps time window.

For a faithful wavelength conversion, the rate of background noises must be sufficiently small compared to that of the converted photons. The background noises are mainly caused by the Raman scattering of the pump light and dark countings of a photon detector. The former is proportional to the pump power and is written by bP with a constant b . The latter is described by a constant d . Taking into account these noise effects and using Eq. (1), the signal-to-noise ratio for the observed converted photons is represented by

$$f_{\text{SNR}}(P) \equiv \frac{a \sin^2(\sqrt{\eta P \tau})}{bP + d}, \quad (2)$$

where a is a constant. When d is comparable to bP as in the case where both detectors D_V and D_T are APDs [7], a maximum of $f_{\text{SNR}}(P)$ is achieved near a pump power P_{max} , which gives the maximum conversion efficiency, and the maximum of $f_{\text{SNR}}(P)$ is close to $f_{\text{SNR}}(P_{\text{max}}) = a/(bP_{\text{max}} + d)$. On the other hand, when d is sufficiently small as in the case of using the SSPDs, we may improve $f_{\text{SNR}}(P)$ significantly by decreasing the pump power. Using $d/b \approx 3.3$ mW in Fig. 2 and $\eta\tau^2 \approx 3.6 \text{ W}^{-1}$ [7], we see that $f_{\text{SNR}}(P)$ reaches its maximum when the pump power is decreased from $P_{\text{max}} \approx 700$ to 50 mW. In the following experiments, we chose the

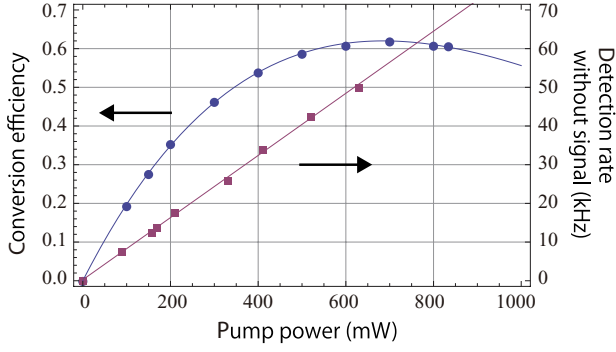


FIG. 2. (Color online) The dependencies of the conversion efficiency and the rate of the background noises on the pump power. The former has been measured by using a picosecond coherent light in Ref. [7]. The latter was measured by using the SSPD for D_T without the UV pulse. The first vertical axis is the conversion efficiency. A maximum conversion efficiency is achieved at a pump power of 700 mW. The second vertical axis is the detection rate of the background noises. We fitted the experimental data by a function of $bP + d$. b and d are estimated as 80 Hz/mW and 266 Hz, respectively.

pump power to be 160 mW for which the conversion efficiency was not severely degraded (about half the maximum value), and the signal-to-noise ratio was expected to be above 10.

Before the wavelength conversion of the entangled photon pairs, we measured the variance of jitter in the arrival time of picosecond photons to see the high timing resolution of the SSPDs. When we used the APDs for both detectors, the full width at half maximum (FWHM) of the time distribution of the coincidence counts was measured to be ≈ 350 ps. When we replaced the InGaAs/InP APD with the SSPD for D_T , the FWHM was measured to be ≈ 290 ps. When we used the SSPDs for both detectors, the FWHM became ≈ 150 ps. These results, shown in Fig. 3, clearly show that the SSPDs gather the coincidence counts in the smaller time bins. The use of the SSPDs, instead of the APDs, is expected to improve the ratio of the signal photons to the optical noises by a factor of about 1.8 in our case of the 200-ps time window.

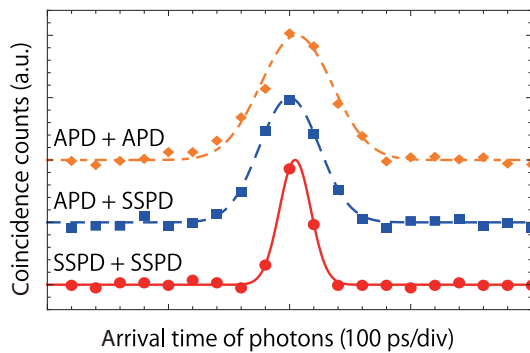


FIG. 3. (Color online) The coincidence counts of the photon pairs recorded by the TDC with the timing resolution of 100 ps when we used rhombuses: the pair of the silicon APDs for D_V and InGaAs/InP APD for D_T ; squares: the silicon APD for D_V and the SSPD for D_T ; and circles: the SSPDs for both the detectors. Each result of the coincidence counts was fitted by the Gaussian function after the subtraction of the counts from the background noises.

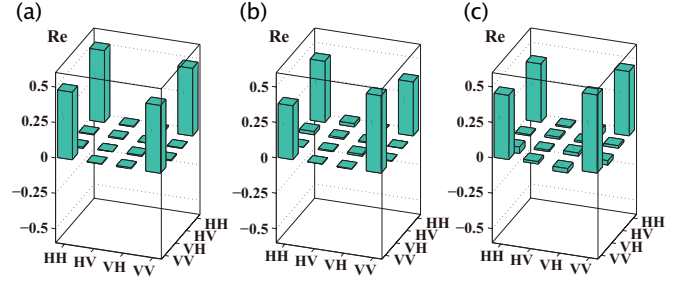


FIG. 4. (Color online) The real parts of the reconstructed density matrices. (a) The initial entangled photon pair ρ_{AB} prepared by the BBO crystal. (b) The two-photon state ρ_{AC}^{AS} after the wavelength conversion when we used the silicon APD for D_V and the SSPD for D_T . (c) The two-photon state ρ_{AC}^{SS} after the wavelength conversion when we used the SSPDs for both detectors D_V and D_T .

In the experiment of the frequency down conversion of the visible entangled photon pairs, we first performed quantum state tomography of the initial photon pairs in modes A and B at 780 nm by rotating a quarter-wave plate (QWP) and a HWP followed by a PBS in each mode [31]. We used a silicon APD for D_V . The PMF, before the frequency down converter, was connected to a silicon APD for the detection of photons in mode B . We observed the two-photon state in modes A and B with a detection rate of 444 Hz. Using the iterative maximum likelihood method [32], the density operator ρ_{AB} was reconstructed as shown in Fig. 4(a). From the reconstructed ρ_{AB} , we calculated the fidelity defined by $\langle \phi^+ | \rho_{AB} | \phi^+ \rangle$, the entanglement of formation (EOF) [33], and the purity defined by $\text{tr}(\rho_{AB}^2)$ as 0.97 ± 0.01 , 0.97 ± 0.03 , and 0.97 ± 0.02 , respectively. These results show that the 780-nm photon pair, before the wavelength conversion, was highly entangled. Next, we performed quantum state tomography of the photon in mode A and the converted photon in mode C' when we used the silicon APD for D_V and the SSPD for D_T . An observed detection rate of the two photons was 0.324 Hz including background noises at a rate of 0.039 Hz. The reconstructed density operator ρ_{AC}^{AS} is shown in Fig. 4(b). The fidelity, EOF, and the purity are shown in Table I. We then switched the silicon APD to the SSPD for D_V and performed quantum state tomography. In this case, we detected the two photons after the conversion at a rate of 0.280 Hz including noise photons at a rate of 0.015 Hz. Assuming the quantum efficiencies 0.32 and 0.125 of SSPDs for photons at

TABLE I. The observed fidelities, the EOFs, the purities, and the S parameters of the reconstructed operators before and after the wavelength conversion. ρ'_{AC} is a reconstructed operator of photons in modes A and C' by using the silicon APD and the InGaAs/InP APD for D_V and D_T , respectively [7]. The attached errors are the standard deviations ($1-\sigma$) with the assumption of the Poisson statistics of the counts.

	F	EOF	Purity	S
ρ_{AB}	0.97 ± 0.01	0.97 ± 0.03	0.97 ± 0.02	2.73 ± 0.02
ρ_{AC}^{AS}	0.87 ± 0.06	0.68 ± 0.15	0.79 ± 0.08	2.35 ± 0.10
ρ_{AC}^{SS}	0.93 ± 0.04	0.88 ± 0.10	0.93 ± 0.07	2.62 ± 0.09
ρ'_{AC} [7]	0.75 ± 0.06	0.36 ± 0.13		

780 and 1522 nm, respectively, and the quantum efficiency 0.6 of the silicon APD, the overall conversion efficiency of photons just before the photon detector is estimated to be about 0.005, which is lower than the value of 0.008 obtained in Ref. [7]. The reconstructed density operator ρ_{AC}^{SS} is shown in Fig. 4(c). The observed fidelity, EOF, and the purity are shown in Table I. We also performed the tests of the Clauser-Horne-Shimony-Holt-type Bell's inequality [34] by observing the S parameter. It is known that any local hidden variable theory leads to $S \leq 2$. The experimental results of the S parameters are shown in Table I. The Bell's inequality was clearly violated with over $6\text{-}\sigma$ deviation. From these results, we see that the high-fidelity frequency down conversion was achieved, which could be more clearly observed with SSPDs.

In conclusion, we have demonstrated the faithful solid-state-based frequency down conversion of visible photons at 780 nm to a telecommunication wavelength of 1522 nm. Thanks to the lower dark count rates and the smaller timing jitters of the SSPDs, the observed fidelity of the two-photon state, after the wavelength conversion, is 0.93 ± 0.04 , which

is much closer to the noiseless conversion than 0.75 ± 0.06 in the previous experiment [7]. On the other hand, the overall conversion efficiency of 0.005 is lower than 0.008 in the previous experiment [7] due to the use of a lower pump power. One of the possible solutions to avoid the pump power suppression is to perform photon detection with a better time resolution, which is, for example, realized by novel detectors reported in Ref. [35]. Our demonstration shows the possibility of a noiseless and wideband solid-state-based frequency down conversion. We believe that such a quantum interface is vital for building quantum networks based on repeaters and for performing various quantum communication protocols.

This work was supported by the Funding Program for World-Leading Innovative R & D on Science and Technology (FIRST), MEXT Grant-in-Aid for Scientific Research on Innovative Areas Grants No. 20104003 and No. 21102008, the MEXT Global COE Program, and MEXT Grant-in-Aid for Young scientists(A) Grant No. 23684035.

-
- [1] P. Kumar, *Opt. Lett.* **15**, 1476 (1990).
 [2] S. Tanzilli *et al.*, *Nature (London)* **437**, 116 (2005).
 [3] H. Takesue, *Phys. Rev. Lett.* **101**, 173901 (2008).
 [4] M. T. Rakher, L. Ma, O. T. Slattery, X. Tang, and K. A. Srinivasan, *Nat. Photonics* **4**, 786 (2010).
 [5] H. J. McGuinness, M. G. Raymer, C. J. McKinstrie, and S. Radic, *Phys. Rev. Lett.* **105**, 093604 (2010).
 [6] Y. O. Dudin *et al.*, *Phys. Rev. Lett.* **105**, 260502 (2010).
 [7] R. Ikuta *et al.*, *Nat. Commun.* **2**, 537 (2011).
 [8] S. Ramelow, A. Fedrizzi, A. Poppe, N. K. Langford, and A. Zeilinger, *Phys. Rev. A* **85**, 013845 (2012).
 [9] S. Zaske *et al.*, *Phys. Rev. Lett.* **109**, 147404 (2012).
 [10] S. Ates, I. Agha, A. Badolato, and K. Srinivasan, *Phys. Rev. Lett.* **109**, 147405 (2012).
 [11] H.-J. Briegel, W. Dür, J. I. Cirac, and P. Zoller, *Phys. Rev. Lett.* **81**, 5932 (1998).
 [12] L. M. Duan, M. D. Lukin, J. I. Cirac, and P. Zoller, *Nature (London)* **414**, 413 (2001).
 [13] N. Gisin and R. Thew, *Nat. Photonics* **1**, 165 (2007).
 [14] J. I. Cirac and P. Zoller, *Nature (London)* **404**, 579 (2000).
 [15] D. N. Matsukevich and A. Kuzmich, *Science* **306**, 663 (2004).
 [16] W. Rosenfeld *et al.*, *Phys. Rev. Lett.* **101**, 260403 (2008).
 [17] C. W. Chou *et al.*, *Nature (London)* **438**, 828 (2005).
 [18] S. Olmschenk *et al.*, *Science* **323**, 486 (2009).
 [19] E. Togan *et al.*, *Nature (London)* **466**, 730 (2010).
 [20] S. Ritter *et al.*, *Nature (London)* **484**, 195 (2012).
 [21] A. Politi, M. J. Cryan, J. G. Rarity, S. Yu, and J. L. O'Brien, *Science* **320**, 646 (2008).
 [22] K. F. Reim *et al.*, *Nat. Photonics* **4**, 218 (2010).
 [23] E. Saglamyurek *et al.*, *Nature (London)* **469**, 512 (2011).
 [24] H. Takesue, *Phys. Rev. A* **82**, 013833 (2010).
 [25] N. Curtz, R. Thew, C. Simon, N. Gisin, and H. Zbinden, *Opt. Express* **18**, 22099 (2010).
 [26] S. Zaske, A. Lenhard, and C. Becher, *Opt. Express* **19**, 12825 (2011).
 [27] S. Miki, M. Takeda, M. Fujiwara, M. Sasaki, and Z. Wang, *Opt. Express* **17**, 23558 (2009).
 [28] S. Miki, T. Yamashita, M. Fujiwara, M. Sasaki, and Z. Wang, *Opt. Lett.* **35**, 2133 (2010).
 [29] T. Yamamoto, K. Hayashi, Ş. K. Özdemir, M. Koashi, and N. Imoto, *Nat. Photonics* **2**, 488 (2008).
 [30] T. Nishikawa *et al.*, *Opt. Express* **17**, 17792 (2009).
 [31] D. F. V. James, P. G. Kwiat, W. J. Munro, and A. G. White, *Phys. Rev. A* **64**, 052312 (2001).
 [32] J. Řeháček, Z. Hradil, E. Knill, and A. I. Lvovsky, *Phys. Rev. A* **75**, 042108 (2007).
 [33] W. K. Wootters, *Phys. Rev. Lett.* **80**, 2245 (1998).
 [34] J. F. Clauser, M. A. Horne, A. Shimony, and R. A. Holt, *Phys. Rev. Lett.* **23**, 880 (1969).
 [35] S. Miki *et al.*, *Appl. Phys. Lett.* **99**, 111108 (2011).